

The comparison of impedance-based method of cell proliferation monitoring with commonly used metabolic-based techniques

Lucie VISTEJNOVA¹, Jana DVORAKOVA¹, Martina HASOVA¹, Tomas MUTHNY¹,
Vladimir VELEBNY¹, Karel SOUCEK², Lukas KUBALA²

¹ CPN spol. s r.o., Czech Republic

² Institute of Biophysics, Academy of Science of the Czech Republic, Brno, Czech Republic

Correspondence to: Lukáš Kubala, Ph.D., Institute of Biophysics, Academy of Sciences of the Czech Republic, Královopolská 135, CZ-612 65 Brno, Czech Republic.
PHONE: +420-541 517 117, FAX: +420-541 211 293, E-MAIL: kupalal@ibp.cz

Submitted: 2009-07-16 *Accepted:* 2009-09-09 *Published online:* 2009-11-15

Key words: fibroblasts; keratinocytes; viability; proliferation; adhesion; luminescence; tetrazolium salt; impedance

Neuroendocrinol Lett 2009; 30(Suppl 1): 121-127 PMID:20027157 NEL300709A20 ©2009NeuroendocrinologyLetters • www.nel.edu

Abstract

OBJECTIVES: Determination of cell numbers is a crucial step in studies focused on cytokinetics and cell toxicity. The impedance-based analysis employing electronic sensor array system xCELLigence System allowing label-free dynamic monitoring of relative viable adherent cell amounts was compared with the most utilized methods for relative quantification of viable cell numbers based on a determination of cellular metabolism.

DESIGN: Colorimetric assay based on reduction of tetrazolium salt (MTT) by mitochondrial enzymes and chemiluminescent assay based on intracellular adenosine triphosphate (ATP) determination were compared with the impedance-based system. Cell morphology was compared by microscopic evaluation. Normal human epidermal keratinocytes (NHEK) and normal human dermal fibroblasts (NHDF), together with 3T3 mouse fibroblast and HaCaT keratinocyte cell lines were employed.

RESULTS: The progress of cell growth curves obtained by different methods during 72 hours reflected cell type and cell seeding densities. The impedance-based method was found to be applicable for the determination of the cell proliferation of 3T3 fibroblasts, HaCaT and NHDF, since the comparison of this method with ATP and MTT determinations showed a comparable results. In contrast, the proliferation of NHEK measured by the impedance-based method did not correlate with other methodological approaches. This could be accounted to the specific morphological appearance of these cells.

CONCLUSION: The study shows the impedance-based detection of viable adherent cells is a valuable approach for cytokinetics and pharmacological studies. However, the specific morphological characteristics of cell lines have to be considered employing this method for determination of cell proliferation without using other reference methods.

Abbreviations & units

| | |
|------|--------------------------------------|
| ATP | adenosine triphosphate |
| DAPI | 4',6-diamidino-2-phenylindole |
| DMEM | Dulbecco's modified Eagle's medium |
| DMSO | dimethyl sulfoxide |
| FBS | fetal bovine serum |
| MTT | methyl thiazolyl tetrazolium |
| NHEK | normal human epidermal keratinocytes |
| NHDF | normal human dermal fibroblasts |
| PBS | phosphate buffered saline |
| SEM | standard error mean |

INTRODUCTION

Currently, the commonly used cell viability assays are: the direct counting of live cells, the quantification of esterase activity, the total nucleic acid mass, the total protein mass, and the cell metabolism (Dong *et al.* 2007; Horvathova *et al.* 2008; Lojek *et al.* 2008). Methods based on the determination of cell metabolism include: the quantification of intracellular adenosine triphosphate (ATP), and the reduction of tetrazolium salts (MTT) to formazan in viable cells. Both of these methodological approaches mirror the amount of active mitochondria (Goodwin *et al.* 1995). The MTT method reflects the activity of mitochondrial dehydrogenases; on the other side, the amount of intracellular ATP directly corresponds to the level of ATP formation in these organelles. Both the colorimetric determination of formazan dyes and the luminiscence determination of ATP employing luciferase provide robust, widely used assays suitable for high-throughput screening (Crouch *et al.* 1993; Petty *et al.* 1995).

However, these methods based on metabolic activity analysis are incompatible with experimental treatments that are directly modulating cellular metabolism, mitochondrial activity, or mitochondria intracellular mass. Further, it has been described that some substances, predominantly redox active compounds, directly react with formazan dyes, bringing misleading information on cell viability (Elisia *et al.* 2008). For these reasons, cell viability estimation by MTT and/or ATP based methods is limited, and other approaches are required.

Nowadays, analysis of cell proliferation in a real-time manner could be performed using commercially available impedance-based systems including xCELLigence System (Roche Applied Science, Switzerland). This assay engages an electrical impedance cell sensor technology to measure the level of impedance on the surface of the cell culture plate/well, which corresponds to the extent of the cell-covered area. This label-free method offers a non-invasive approach to the monitoring of cell adhesion, proliferation as well as the role of surface molecules, and the influence of chemicals on the mentioned cell processes (Otto *et al.* 2003; Spiegel *et al.* 2008; Xi *et al.* 2008). The advantages of label-free detection include a simple homogeneous assay format, the possibility of reuse of applied cells, less interference with normal cell function, kinetic measurement, and a reduced time for

assay development. This method, by its nature, depends on the extent of area over which cells are spread, and thus also reflects the morphological properties of cells. Accordingly, any modulation of cell morphology induced by physiological conditions such as an increase of cell-to-cell contact, confluence status, or modulation of cell morphology by different chemicals as applied in pharmacology or toxicology would affect the measured impedance signal (Spegel *et al.* 2008). However, there is little awareness that applying impedance-based determination in pharmacological and toxicological studies for cell proliferation would be strongly dependent on cell type, due to different morphological properties.

In this study, metabolism-based methods of relative cell viability determination have been compared with the impedance-based methodological approach in two types of primary culture skin cells and two corresponding immortalized lines.

MATERIALS AND METHODS

Cell lines. Spontaneously immortalized human keratinocyte cell line HaCaT (a kind gift from Prof. Dr. N. Fusenig, Deutsches Krebsforschungszentrum, Heidelberg, Germany) was grown in Dulbecco's modified Eagle's medium-low glucose (DMEM) (Sigma-Aldrich, USA) supplemented with 10% fetal bovine serum (FBS) (Invitrogen, USA), glutamine (0.3 mg ml⁻¹) (Sigma-Aldrich) and gentamicin (50 µg ml⁻¹) (Invitrogen) in 5.0% CO₂ at 37°C in 75 cm² culture flask (TPP, Switzerland). Swiss albino mouse fibroblasts 3T3 (Deutsche Sammlung von Mikroorganismen und Zellkulturen, Germany, DSMZ No. ACC 173) were grown in DMEM supplemented with 10% FBS, glutamine (0.3 mg ml⁻¹), penicillin (100 U ml⁻¹) (Sigma-Aldrich) and streptomycin (0.1 mg ml⁻¹) (Sigma-Aldrich) in 5.0% CO₂ at 37°C in 75 cm² culture flask as recommended by the supplier. Normal human epidermal keratinocytes (NHEK) were isolated from facial skin removed during cosmetic plastic surgery, under the informed consent of the donor. NHEK cultures were prepared as described previously (Rheinwald & Green, 1975). NHEK were cultivated in DMEM (PAN-Biotech GmbH, Germany) and F-12 Nutrient mixture (Invitrogen) supplemented with 10% FBS, hydrocortisone (0.35 µg ml⁻¹), adenine (0.031 mg ml⁻¹), cholera toxin (0.85 ng ml⁻¹), EGF (epidermal growth factor) (1.0 ng ml⁻¹), insulin (5 µg ml⁻¹), apotransferrin (2.5 µg ml⁻¹) and 3,3,5-tri-iodo-L-thyronine (0.7 ng ml⁻¹) (all from Sigma-Aldrich) and antibiotic mixture (penicillin 20 U ml⁻¹, streptomycin 20 µg ml⁻¹, amphotericin B 0.05 µg ml⁻¹) (Invitrogen). NHEK were cultivated until 70–90% confluence and then sub-cultivated and grown in 7.5% CO₂ at 37°C in 75 cm² culture flasks. (Frankova *et al.* 2006; Ruzova *et al.* 2008). Normal human dermal fibroblasts (NHDF) were also isolated from facial skin removed during cosmetic plastic surgery. NHDF were obtained from dermis by migration or digestion methods (Meske *et al.*

2005). NHDF were cultured in DMEM supplemented with 10% FBS, glutamine (0.3 mg ml^{-1}), glucose (4 mg ml^{-1}) (Lach-Ner, Czech Republic), penicillin (100 U ml^{-1}) and streptomycin (0.1 mg ml^{-1}) in 7.5% CO_2 at 37°C in 75 cm^2 culture flasks. Primary cell lines were cultured till 2nd–3rd passage. Cells were seeded on 96 well test plates (TPP) for MTT and ATP, or on 96 well E-plates (Roche Applied Science, Switzerland) for impedance in the volume of 200 μl . The seeding cell density was $5\,000$ – $30\,000 \text{ cells cm}^{-2}$. All samples were seeded in triplicates, and blank samples were included. The cells were let to adhere overnight, and the cell viability assays were carried out at different time-points. The experiments were repeated at least three times in their entirety.

Colorimetric assay (MTT). The MTT assay was carried out according to manufacturer instructions (Sigma-Aldrich). Briefly, 20 μl of MTT work solution (5 mg ml^{-1}) was added to each well and incubated at 37°C , 7.5% CO_2 for 2 hours. The medium was removed and the cells were lysed in 220 μl of lysis solution (isopropylalcohol : DMSO 1:1, Triton-X, HCl) for 30 min. The optical density was measured every 24 hours at 570 nm using a Versa Max Microplate Reader (Molecular Devices, Sunnyvale, CA, USA) and corrected by the 690 nm reference wavelength.

Chemiluminescent assay (ATP). The culture medium was replaced with 100 μl media with 20 μl of CellTiter-Glo[®] reagent (Promega, USA) and shaken for 30 minutes. Afterwards, cell lysate was let stand for 5 minute to equilibrate the luminiscence signal. 100 μl of cell lysate was placed onto a black 96well test plate (NUNC, Denmark), and the luminiscence signal was measured every

24 hours by a Fluorescent reader INFINITE M200 (Tecan Group Ltd., Switzerland).

Impedance-based assay. Impedance analyses were carried out using the xCELLigence System (Roche Applied Science) in E-Plates 96 (Roche Applied Science), according to the manufacturer's instructions. Briefly, the background signal of culture medium was set up in E-plate, firstly. The cells were seeded into E-plate in 200 μl culture medium and signal was measured every 3 minutes for 72 hours, immediately after the seeding.

Cell culture staining. Cells were seeded in concentration 10 000 and 20 000 cells per cm^2 into 2 cm^2 wells and cultured for 72 hours. Cells were washed with phosphate buffered saline (PBS), fixed in 2.5% formaldehyde in PBS for 5 minutes, washed with PBS, and permeabilized by methanol. Cells were washed and F-actin and cell nuclei were stained with fluorescein-labelled phalloidin ($20 \mu\text{g ml}^{-1}$) and DAPI ($0.1 \mu\text{g ml}^{-1}$) in PBS (both from Sigma-Aldrich) at 4°C for 1 h, respectively. Cells were washed twice with PBS, mounted, F-actin and cell nuclei were visualised using a fluorescent microscope (Olympus IX-70, Fluoview II CCD camera), and cell morphology was documented on the same microscope by phase-contrast.

Statistical analysis. At least three independent repeats were performed for each experimental setup. All data are reported as means \pm standard error of mean (SEM). Pearson's correlation coefficients were calculated for detected signal, cell seeding density, and time period of cell cultivation (Microsoft Office Excel 2003).

Table 1. The Pearson's correlation coefficients describing the correlation of signal value and the time course. The mean values of Pearson's coefficient obtained in three independent experimental repeats are shown, supplied with SEM.

| cells cm^2 | HaCaT | | | NHEK | | |
|---------------------|-----------------|-----------------|------------------|-----------------|-----------------|------------------|
| | MTT | ATP | Imp | MTT | ATP | Imp |
| 5 000 | 0.89 ± 0.09 | 0.96 ± 0.01 | 0.98 ± 0.00 | 0.55 ± 0.42 | 0.95 ± 0.01 | -0.24 ± 0.12 |
| 10 000 | 0.99 ± 0.01 | 0.93 ± 0.06 | 0.99 ± 0.01 | 0.60 ± 0.39 | 0.90 ± 0.06 | -0.30 ± 0.31 |
| 15 000 | 0.88 ± 0.10 | 0.99 ± 0.01 | 0.93 ± 0.06 | 0.39 ± 0.58 | 0.84 ± 0.08 | 0.07 ± 0.42 |
| 20 000 | 0.97 ± 0.02 | 0.96 ± 0.01 | 0.88 ± 0.11 | 0.43 ± 0.55 | 0.51 ± 0.41 | -0.37 ± 0.18 |
| 25 000 | 0.95 ± 0.03 | 0.84 ± 0.08 | 0.65 ± 0.22 | 0.44 ± 0.55 | 0.80 ± 0.12 | -0.27 ± 0.34 |
| 30 000 | 0.75 ± 0.13 | 0.87 ± 0.08 | 0.69 ± 0.23 | 0.63 ± 0.25 | 0.99 ± 0.00 | -0.05 ± 0.14 |
| cells cm^2 | 3T3 | | | NHDF | | |
| | MTT | ATP | Imp | MTT | ATP | Imp |
| 5 000 | 0.77 ± 0.21 | 0.90 ± 0.03 | -0.30 ± 0.58 | 0.96 ± 0.01 | 0.94 ± 0.04 | 0.96 ± 0.01 |
| 10 000 | 0.92 ± 0.04 | 0.96 ± 0.03 | 0.91 ± 0.06 | 0.83 ± 0.17 | 0.89 ± 0.04 | 0.98 ± 0.00 |
| 15 000 | 0.79 ± 0.19 | 0.93 ± 0.02 | 0.99 ± 0.01 | 0.98 ± 0.46 | 0.95 ± 0.03 | 1.00 ± 0.00 |
| 20 000 | 0.86 ± 0.01 | 0.96 ± 0.03 | 0.95 ± 0.00 | 0.99 ± 0.00 | 0.95 ± 0.02 | 1.00 ± 0.00 |
| 25 000 | 0.85 ± 0.01 | 0.94 ± 0.01 | 0.95 ± 0.01 | 0.90 ± 0.05 | 0.93 ± 0.04 | 1.00 ± 0.00 |
| 30 000 | – | – | 1.00 ± 0.00 | 0.90 ± 0.09 | 0.99 ± 0.00 | 0.99 ± 0.00 |

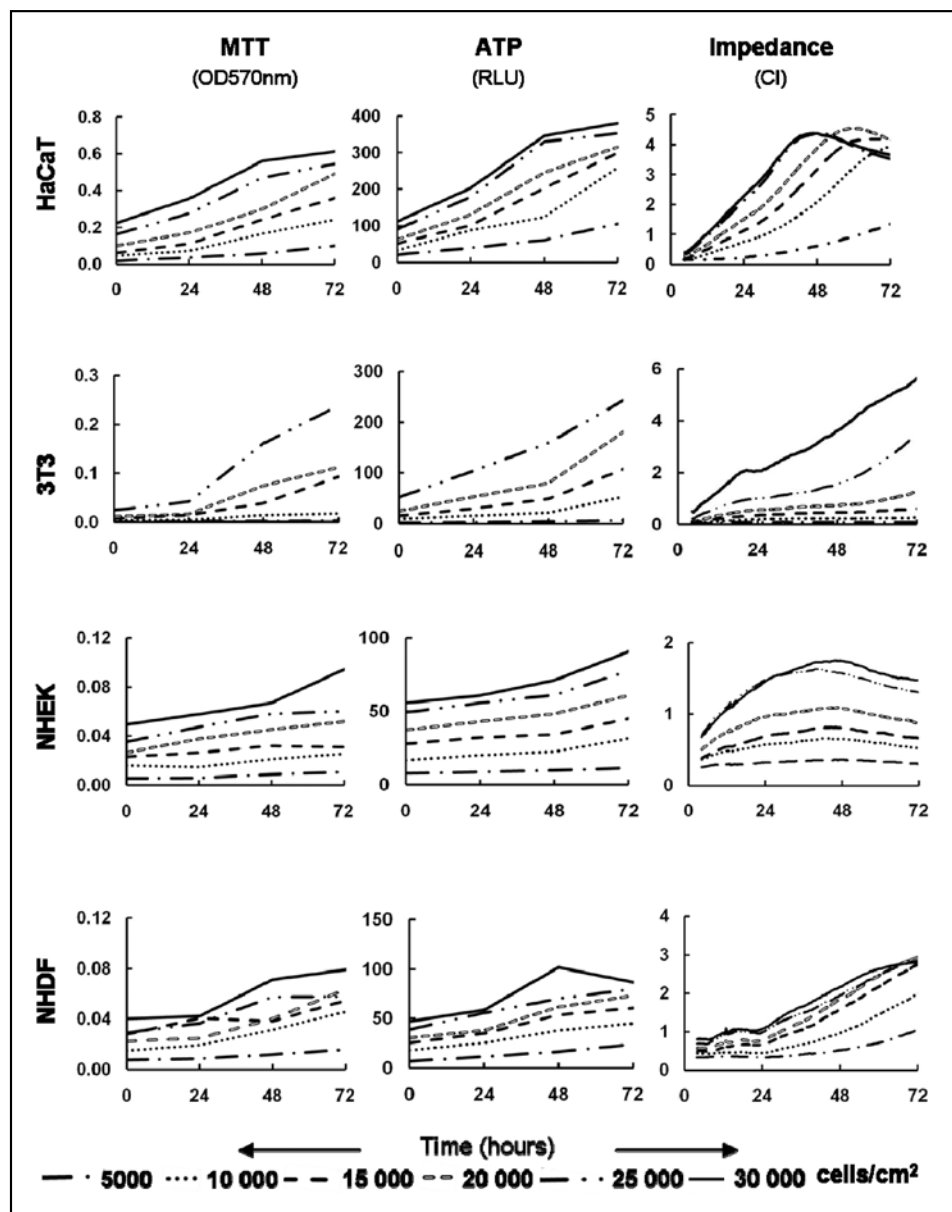


Figure 1. Growth curves of four cell types measured by three methods – formazan detection, ATP detection, and the impedance-based method. The cells were seeded at densities 5 000–30 000 cells/cm² and left to adhere overnight; the examinations were carried out 24 hours after seeding and in the following 24-hour intervals. Curves represent the means of values of detected signal done from three independent repeats. (OD = optical density, RLU = relative luminiscence units, CI = cell index)

RESULTS

The methodological approach based on impedance measurement was compared with the measurement of intracellular ATP and formazan reduction for determination of proliferation of fibroblasts and keratinocytes in concentration range 5 000 – 30 000 cells per cm² over a period of 72 h. Each cell type revealed its own curve shape, which was dependent on cell characteristics, seeding density, and a particular method (**Fig. 1**). The shape of curves obtained from the determination of cell proliferation by the impedance-based method showed an increasing trend for all cell types, except for keratinocytes, in which case even a slight decrease in the detected signal was observed.

To further describe a linear relation between the relative signal obtained from each method and the number of seeded cells, Pearson's correlation coefficients were

determined for each cell type and method. There was a very good correlation in most sample sets. The highest coefficients were obtained at 24 hours after seeding (all correlation coefficients were over 0.91). At 48 and 72 hours after seeding, slightly lower coefficients were obtained (all correlation coefficients were over 0.88 and 0.75, respectively).

The correlation of the value of signal and the time course (24, 48, 72 hours) was expressed using the Pearson's correlation coefficient. The coefficients were determined for all seeding densities, methods and cell types (**Table 1**). All coefficients for NHDF were very high for all seeding densities and methods. The correlation coefficients for the HaCaT cell line were very high till 20 000 cells/cm². Both cell types displayed linear progress over time. In the case of 3T3 fibroblasts, there was a satisfactory correlation between the values in all data sets, with an exception of the impedance-based

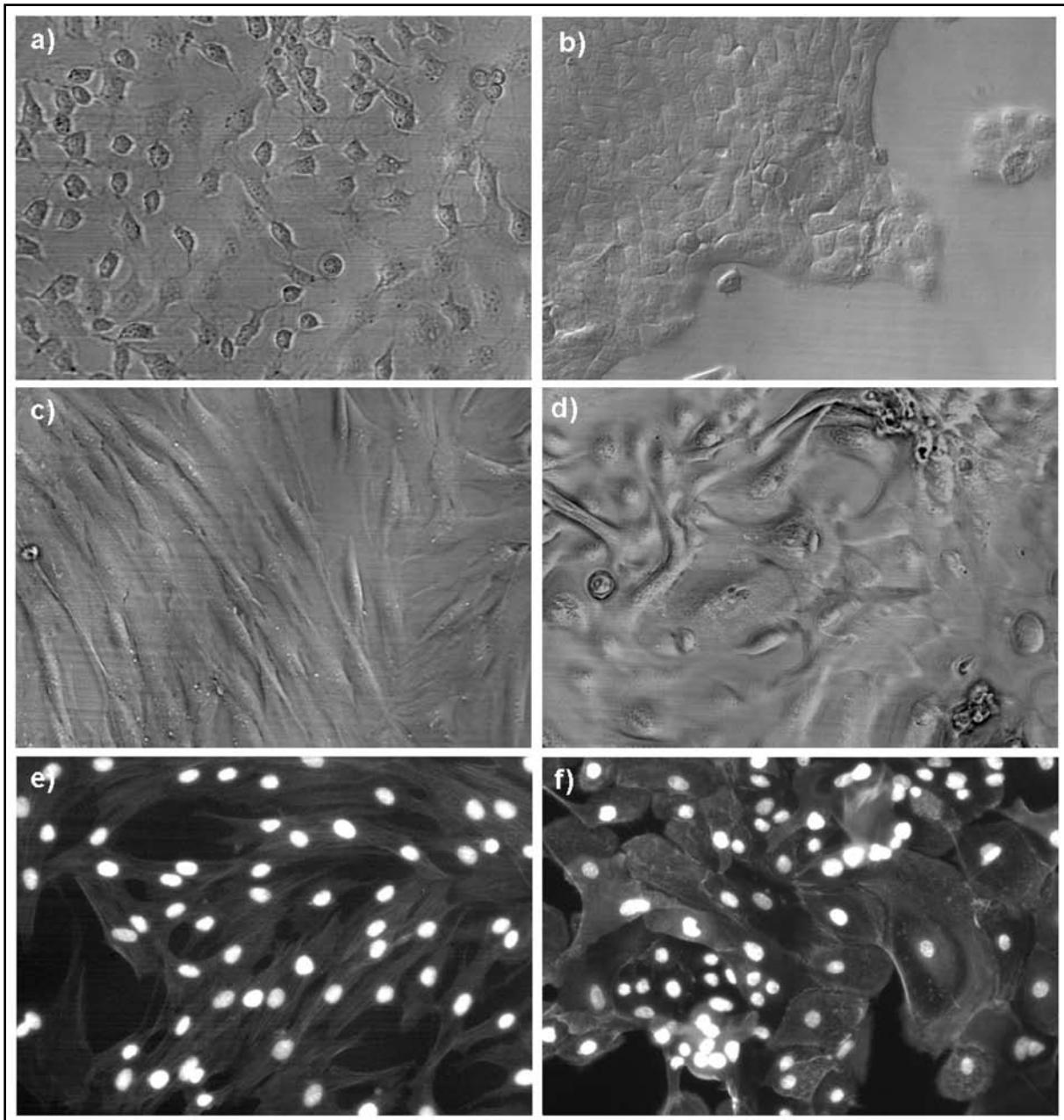


Figure 2. Phase contrast (a-d) and phalloidin/DAPI (e, f) pictures of 3T3 (a), NHDF (c, e), HaCaT (b) and NHEK (d, f) after 72-hour cultivation are shown. Both types of fibroblasts and HaCaT cell line cover the plate surface as a monolayer, whereas NHEK tend to overlap each other and create gaps in the cell layer (original magnification 10x).

method at the lowest seeding density. Interestingly, the impedance-based method completely failed to mirror the proliferation of NHEK over time. In comparison, the ATP values reflected the linear progress at the most seeding densities, and the MTT correlation coefficients show a low degree of linearity in MTT values over the incubation time.

To clarify the discrepancy between the metabolic activity of NHEK and the impedance measurements, morphological differences among cell lines and morphological changes during cell proliferation from the time of seeding up to the confluent layer of cells was evaluated using phase contrast microscopy and phalloi-

din labelling of the actin cytoskeleton. Morphological analysis showed that 3T3 (**Fig. 2a**) and NHDF (**Fig. 2c, e**) cells grow in a circle or spindle shape, respectively, and form a regular cell monolayer. A similar situation can be seen with the HaCaT cell line (**Fig. 2b**), which grows in a cobble-stone shape and gives rise to one flat layer of tightly connected cells. In contrast, NHEK are of a polygonal shape; and, with increased confluence, they grow irregularly, with significant overlapping within proximal cells and together with the uncovered spaces that appear between cells. In later stages of growth, the cells are distributed in patches, and tend to grow over each other (**Fig. 2d, f**).

DISCUSSION

The impedance-based method for assessment of cell proliferation was shown to be comparable with other methods based on determination of cell metabolism in both fibroblast primary culture (NHDF) and cell line (3T3) and immortalized human keratinocytes HaCaT. On the other side, NHEK proliferation monitored by metabolic activity and by impedance did not significantly associate. Cell morphology analysis of NHEK showed that this phenomenon could reside in the different growth patterns of these cells.

The assessment of cell proliferation by the impedance method is applicable to adherent cells and the method is based on the assumptions that current flows radially through the growth surface (the plastic plate with electrode surface) between cells and through the junctions between adjacent cells (Bik *et al.* 2008; Giaever & Keese 1991; Heiskanen *et al.* 2008; Ye *et al.* 2003). Previously, a high correlation between impedance-based determination of viable adherent cells and MTT determination was described in macrophages (Zhu *et al.* 2006), 3T3 fibroblasts (Ceriotti *et al.* 2007; Xing *et al.* 2005), Chinese hamster ovarian cells K1 (Xing *et al.* 2005), H1080 human fibrosarcoma cell line (Atienza *et al.* 2006), and H460 adenocarcinoma cell line (Atienza *et al.* 2006). However, these experiments mostly focused on short-term tests up to 24 h and were designed for cytotoxic studies that did not follow an increase of impedance, but rather a decrease of impedance based on cell dying (Ceriotti *et al.* 2007; Kirstein *et al.* 2006; Xi *et al.* 2008; Xing *et al.* 2005). Interestingly, in some cases these authors even observed a transient increase of cell impedance after the addition of highly toxic compounds, which did not mirror an increase of cell numbers but a transient change in cell morphology, as was shown by the evaluation of cell morphology (Xing *et al.* 2005). No other systematic comparison of the impedance-based determination of cell proliferation with conventional metabolic-based assays has ever been conducted. This study has shown that these methods provide comparable results in longer time periods, up to 72 hours for most cell types.

As was suggested previously, each cell type has its own unique signature pattern of attachment and growth, as demonstrated by the kinetic trace of the cell index curves as observed by the impedance-based technique (Xing *et al.* 2005). The characteristics of the trace are determined by the number of cells seeded, the overall size and morphology of the cells, and the degree to which the cells interact with the sensor surface (Atienza *et al.* 2006; Bik *et al.* 2008). In this study, the metabolic assays did not accord with impedance-based method when employing NHEK. The impedance-based method assumes that the current density between the growth surface and the cells does not change in the vertical direction and the height of the space between the electrode and the lower cell membrane (Heiskanen

et al. 2008). These factors are generally dependent on changes in cellular morphology as well as interaction between the growth substrate and the cells. Both fibroblast cell lines and HaCaT evenly covered the surface of the cell culture plate from single cells to confluent cell layer. The cellular shape and the array of the particular cell cover did not significantly change from single cell stage to confluent layer. In contrast, NHEK grew over each other with uneven morphology forming both short and long membrane protrusive structures that attach the cell culture plate. Thus, we could speculate that the discrepancy between the impedance signal and cell metabolism, together with the visually increasing number of cells during the incubation period, was due to the irregular grown pattern of NHEK. This assumption is supported by authors who applied an impedance-based method for determination of transient and permanent changes in cell morphology (Atienza *et al.* 2006; Bik *et al.* 2008; Heiskanen *et al.* 2008; Reddy *et al.* 1998; Xing *et al.* 2005). Recently, for their cell impedance applications, most of the authors predominantly employed cells that show good adherence to the growth surface and form tight junctions to the adjacent cells, e.g., fibroblasts, making them an appropriate model for applications relying on impedance measurements (Heiskanen *et al.* 2008). However, cells that are poorly adherent give a low response in impedance measurements, which complicates long-term monitoring of proliferation, as was reported of poorly adherent cells PC-12 (Slaughter *et al.* 2004). Our data further support the notion that the application of the impedance-based method to access cell proliferation is also problematic in cell lines which do not form a regular single cell layer over the culture wells.

The impedance-based method was found to be applicable for determination of cell proliferation in fibroblast cell lines and HaCaT cell line over a wide range of cell concentrations. However, our data suggest that the impedance-based method is not suitable for the determination of the cell proliferation of cells with uneven cellular growth morphological patterns, particularly NHEK. The use of the impedance-based method for high throughput screening in drug discovery should be preceded by a careful evaluation of cell morphology, especially in long-term experiments. A valuable application of this method could lie in toxicology research employing compounds that react with MTT and bring artificial results.

Acknowledgements

Lukas Kubala was supported by grants AVOZ50040507 and AVOZ50040702 (Academy of Sciences of the Czech Republic), OC08058 (MEYS of the Czech Republic) and 524/08/1753 (Czech Science Foundation).

REFERENCES

- 1 Atienza JM, Yu N, Kirstein SL, Xi B, Wang X, Xu X, et al (2006). Dynamic and label-free cell-based assays using the real-time cell electronic sensing system. *Assay Drug Dev Technol.* **4**: 597–607.
- 2 Bik W, Skwarlo-Sonta K, Szelagiewicz J, Wolinska-Witort E, Chmielowska M, Martynska L, et al (2008). Involvement of the cocaine-amphetamine regulated transcript peptide (CART 55-102) in the modulation of rat immune cell activity. *Neuroendocrinol Lett.* **29**: 359–365.
- 3 Ceriotti L, Kob A, Drechsler S, Ponti J, Thedinga E, Colpo P, et al (2007). Online monitoring of BALB/3T3 metabolism and adhesion with multiparametric chip-based system. *Anal Biochem.* **371**: 92–104.
- 4 Ceriotti L, Ponti J, Colpo P, Sabbioni E, Rossi F (2007). Assessment of cytotoxicity by impedance spectroscopy. *Biosens Bioelectron.* **22**: 3057–3063.
- 5 Crouch SP, Kozlowski R, Slater KJ, Fletcher J (1993). The use of ATP bioluminescence as a measure of cell proliferation and cytotoxicity. *J Immunol Methods.* **160**: 81–88.
- 6 Dong XF, Song Q, Li LZ, Zhao CL, Wang LQ (2007). Histone deacetylase inhibitor valproic acid inhibits proliferation and induces apoptosis in KM3 cells via downregulating VEGF receptor. *Neuroendocrinol Lett.* **28**: 775–780.
- 7 Elisia I, Popovich DG, Hu C, Kitts DD (2008). Evaluation of viability assays for anthocyanins in cultured cells. *Phytochem Anal.* **19**: 479–486.
- 8 Frankova J, Kubala L, Velebny V, Ciz M, Lojek A (2006). The effect of hyaluronan combined with KI3 complex (Hyiodine wound dressing) on keratinocytes and immune cells. *J Mater Sci Mater Med.* **17**: 891–898.
- 9 Giaever I, Keese CR (1991). Micromotion of mammalian cells measured electrically. *Proc Natl Acad Sci U S A.* **88**: 7896–7900.
- 10 Goodwin CJ, Holt SJ, Downes S, Marshall NJ (1995). Microculture tetrazolium assays: a comparison between two new tetrazolium salts, XTT and MTS. *J Immunol Methods.* **179**: 95–103.
- 11 Heiskanen AR, Spegel CF, Kostesha N, Ruzgas T, Emneus J (2008). Monitoring of *Saccharomyces cerevisiae* cell proliferation on thiol-modified planar gold microelectrodes using impedance spectroscopy. *Langmuir.* **24**: 9066–9073.
- 12 Horvathova E, Eckl PM, Bresgen N, Slamenova D (2008). Evaluation of genotoxic and cytotoxic effects of H₂O₂ and DMNQ on freshly isolated rat hepatocytes; protective effects of carboxymethyl chitin-glucan. *Neuroendocrinol Lett.* **29**: 644–648.
- 13 Kirstein MN, Brundage RC, Elmquist WF, Remmel RP, Marker PH, Guire DE, et al (2006). Characterization of an in vitro cell culture bioreactor system to evaluate anti-neoplastic drug regimens. *Breast Cancer Res Treat.* **96**: 217–225.
- 14 Lojek A, Pecivova J, Macickova T, Nosal R, Papezikova I, Ciz M (2008). Effect of carvedilol on the production of reactive oxygen species by HL-60 cells. *Neuroendocrinol Lett.* **29**: 779–783.
- 15 Meske V, Albert F, Ohm TG (2005). Cell cultures of autopsy-derived fibroblasts. *Methods Mol Med.* **107**: 111–123.
- 16 Otto AM, Brischwein M, Niendorf A, Henning T, Motrescu E, Wolf B (2003). Microphysiological testing for chemosensitivity of living tumor cells with multiparametric microsensor chips. *Cancer Detect Prev.* **27**: 291–296.
- 17 Petty RD, Sutherland LA, Hunter EM, Cree IA (1995). Comparison of MTT and ATP-based assays for the measurement of viable cell number. *J Biolumin Chemilumin.* **10**: 29–34.
- 18 Reddy L, Wang HS, Keese CR, Giaever I, Smith TJ (1998). Assessment of rapid morphological changes associated with elevated cAMP levels in human orbital fibroblasts. *Exp Cell Res.* **245**: 360–367.
- 19 Rheinwald JG, Green H (1975). Serial cultivation of strains of human epidermal keratinocytes: the formation of keratinizing colonies from single cells. *Cell.* **6**: 331–343.
- 20 Ruzsova E, Pavek S, Hajkova V, Jandova S, Velebny V, Papezikova I, et al (2008). Photoprotective effects of glucomannan isolated from *Candida utilis*. *Carbohydr Res.* **343**: 501–511.
- 21 Slaughter GE, Bieberich E, Wnek GE, Wynne KJ, Guiseppe-Elie A (2004). Improving neuron-to-electrode surface attachment via alkanethiol self-assembly: an alternating current impedance study. *Langmuir.* **20**: 7189–7200.
- 22 Spegel C, Heiskanen A, Pedersen S, Emneus J, Ruzgas T, Taboryski R (2008). Fully automated microchip system for the detection of quantal exocytosis from single and small ensembles of cells. *Lab Chip.* **8**: 323–329.
- 23 Starsikova A, Kubala L, Lincova E, Pernicova Z, Kozubik A, Soucek K (2009). Dynamic monitoring of cellular remodeling induced by the transforming growth factor - beta1. *Biological Procedures Online*. In Press. Article DOI: 10.1007/s12575-009-9017-9
- 24 Xi B, Yu N, Wang X, Xu X, Abassi YA (2008). The application of cell-based label-free technology in drug discovery. *Biotechnol J.* **3**: 484–495.
- 25 Xing JZ, Zhu L, Jackson JA, Gabos S, Sun XJ, Wang XB, et al (2005). Dynamic monitoring of cytotoxicity on microelectronic sensors. *Chem Res Toxicol.* **18**: 154–161.
- 26 Ye JS, Ottova A, Tien HT, Sheu FS (2003). Nanostructured platinum-lipid bilayer composite as biosensor. *Bioelectrochemistry.* **59**: 65–72.
- 27 Zhu J, Wang X, Xu X, Abassi YA (2006). Dynamic and label-free monitoring of natural killer cell cytotoxic activity using electronic cell sensor arrays. *J Immunol Methods.* **309**: 25–33.